IJICTR
International Journal of Information & Communication Technology Research

Volume 14- Number 4 – 2022 (36 -45)

Digital Image Enhancement Through Bi-Histogram Equalization Using Entropy-Based Plateau Limit

Vida Safardoulabi
Department of Computer Engineering
South Tehran Branch, Islamic Azad University
Tehran, Iran
st_v_safardoulabi@azad.ac.ir

Kambiz Rahbar*
Department of Computer Engineering
South Tehran Branch, Islamic Azad University
Tehran, Iran
k_rahbar@azad.ac.ir

Received: 5 July 2022 – Revised: 30 September 2022 - Accepted: 20 October 2022

Abstract—**The equalization of histograms is a simple and efficient process for contrast enhancement. This paper presents equalization of the bi-histogram with the level of the entropy-based plateau. In the first step, the input histogram is divided into two separate sub-histograms, using the mean brightness as a primary threshold of total image pixels. The mentioned threshold is updated in a way that it minimizes the different values of discrete entropy between each section. Then, based on the measured plateau value, these sub-histograms are clipped to prevent unnecessary enhancement. Finally, the image intensity is stretched based on the cumulative distribution function. Laboratory results show that this method gives better outcomes of enhancement, especially in the presence of noise, compared to some two-section methods of preserving of brightness of the histogram equalization.**

Keywords: Bi-Histogram equalization; Image contrast enhancement; Brightness preservation; Discrete Entropy.

Article type: Research Article

I. Introduction

Many features of the visual image can be amplified through contrast correction. The quality of extracted feature vectors might also be affected through contrast correction as well. However, the contrast correction process would not always lead to the expected result. For example, it is possible that the illumination function distribution changes in an unacceptable way [1]–[4]. One of the most difficult aspects of this field is preserving the quality of image's physical edge. Preserving the quality of image physical edge is one of the challenging aspects in this field [5]–[10]. The procedure for extracting contrast correction transfer function is generally defined based on cumulative distribution function of the image. Having too many pixels with the same illumination in an image could lead to increasing the level of contrast correction transfer function, which is known as intensity level saturation.

The methods for image contrast correction are generally divided into two groups: global [10]–[15] and local [2]–[4], [9], [16]–[22]. One of the major disadvantages of the global method is intensity level

* Corresponding Author

[DOI: 10.52547/itrc.14.4.36]

saturation, which leads to dismissing the image information. It also causes the produced image to lose its natural quality. Intensity level saturation is often controlled by controlling the average illumination level of the image[9], [23]–[25]. In other words, it is tried to treat the contrast correction in a way to keep the value of average illumination intensity of the image constant before and after correction.

The methods which are provided based on the rule of preserving illumination tension, at first divide the image histogram into two or more sections. Then, the histogram equalization process would be carried out for each section separately. The discrimination aspect of these methods is generally the criteria based on which the image histogram is divided. The [5], [25], and[37] methods are some samples of the field. Using the mean or median of illumination tension value in an image is one of the common criteria for dividing the image histogram. Another disadvantage of the global method is that it amplifies amplifying the noise in the image simultaneously. The dominant approach to controlling the noise amplification in the image during the process of histogram correction is histogram clipping. Employing the average illumination intensity in each section is the simplest current technique in the field, which clips the probability distribution values based on the average value of that section. Then, considering the clipped value, the probability cumulative function is calculated in order to control the contrast. In the new approaches to calculating the clipped value, discrete entropy used.[1], [24], [38], and[42] can be mentioned as an example. In the present paper, the image contrast enhancement is done based on three main steps. First, the histogram of the input image is calculated and divided into two sub-histograms based on threshold T. The threshold T is calculated using the average values of image total illumination and corrected in a way to minimize the different value of discrete entropy between each section. Second, to prevent unnecessary enhancement, due to the consideration of the measured plateau value, the sub-histograms are clipped Third, the image intensity is stretched based on the cumulative distribution function. This paper is organized as follows: in section II, the proposed method is explained. In section III the laboratory results are explained, and in section IV is devoted to the conclusion.

II. Clipped Entropy-based Bi-Histogram Equalization

The histogram $h(x)$ for intensity x, in a given image $X$is provided as:

$$h(x) = n_x, \quad \text{for } x = 0, 1, \dots, L-1 \tag{1}$$

Where the number of occurrences of intensity xin the image is signified by n_x and the brightness gray level is signified by $L-1$. The following equation is provided for the probability density function, $p(x)$.

$$p(x) = \frac{h(x)}{N}, \quad \text{for } x = 0, 1, \dots, L-1 \tag{2}$$

Here, Nis the total number of pixels in the image. The following equation (3) is presented for the cumulative density function, $c(x)$.

$$c(x) = \sum_{k=X_0}^{x} p(k) \tag{3}$$

The input image is mapped into the entire dynamic range, $[X_0, X_{L-1}]$, through the transformation function $f(x)$ for the standard histogram equalization by using $c(x)$. The following equation is provided for this process.

$$f(x) = X_0 + (X_{L-1} - X_0).c(x) \tag{4}$$

Using equation 4, the output image ($Y = \{Y(i,j)\}$) histogram equalization, can be presented as:

$$Y = \{Y(i,j)\} = \{f(x(i,j) | \forall X(i,j) \in X\} \tag{5}$$

Where (i,j) is the special coordinate of the pixel in the image.

To describe the methodology of Clipped Bi-Histogram Equalization, first, the intensity threshold (X_T) is defined to decompose the input image into two sub-images X_L and X_U. The primary threshold X_T defined as the mean value of the total illumination image. Next, its value is updated iteratively in a way to minimize the different values of discrete entropy between each image section. Then two plateau limits T_L and T_U as given in (6) and (7), are defined to clip the histograms of two sub-images h_L and h_U.

$$T_L = \frac{E_L}{E_T} \cdot \frac{1}{X_T + 1} \sum_{k=0}^{X_T} h_L(k) \tag{6}$$

$$T_U = \frac{E_U}{E_T} \cdot \frac{1}{(L-1) - X_T} \sum_{k=X_T+1}^{L-1} h_U(k) \tag{7}$$

Where E_T is the input image discrete entropy and E_L and E_U are discrete entropy of X_L and X_U respectively as given in 8.

$$E_i(x) = -\sum_{k=u}^{v} p_i(k) \log_2(p_i(k)), \quad \forall i \in U, L, T \tag{8}$$

Where u and vare the minimum and maximum gray level, respectively, of the image X. Next, in order to control the enhancement rate of contrast enhancement, sub-histograms h_L and h_U are clipped as given in (9) and (10).

$$h_{cL}(x) = \begin{cases} h_L(x) & \text{if } h_L(x) \le T_L \\ T_L & \text{if } h_L(x) > T_L \end{cases} \tag{9}$$

$$h_{cU}(x) = \begin{cases} h_U(x) & \text{if } h_U(x) \le T_U \\ T_U & \text{if } h_U(x) > T_U \end{cases} \tag{10}$$

Then, $p_{cL}(x)$ and $p_{cU}(x)$, the probability density functions for two sub-images X_L and X_U are calculated by:

$$p_{cL}(x) = \frac{h_{cL}(x)}{N_L}, \quad \text{for } x = 0, 1, \dots, X_T \tag{11}$$

$$p_{cU}(x) = \frac{h_{cU}(x)}{N_U}, \quad \text{for } x = X_T + 1, X_T + 2, \dots, L-1 \tag{12}$$

N_L and N_U are the total number of pixels intwo sub-images $\boldsymbol{X}_L$ and $\boldsymbol{X}_U$ respectively. Next, the respective cumulative density functions for $\boldsymbol{X}_L$ and $\boldsymbol{X}_U$ are defined by using (13) and (14).

[DOI: 10.52547/itrc.14.4.36]

$$c_{cL}(x) = \sum_{k=X_0}^{X_T} p_{cL}(k) \quad (13)$$

$$c_{cU}(x) = \sum_{k=X_T+1}^{L-1} p_{cU}(k) \quad (14)$$

The transformation function f(x) for the clipped bi-histogram equalization is given by the following equation.

$$f(x) = \begin{cases} X_0 + (X_T - X_0).c_{cL}(x) \\ X_{T+1} + (X_{L-1} - X_{T+1}).c_{cU}(x) \end{cases} \quad (15)$$

The above transformation function does not preserve edges of the image. To preserve edges, the guided filter was introduced by [5] as an edge-preserving smoothing operator. A guided filter is an explicit image filter derived from a local linear model considering the content of a guidance image [8]. So, the equation 15 modified as bellow.

$$f(x) = \begin{cases} X_0 + (X_T - X_0).\{c_{cL}(x) + [\frac{X - X_0}{X_T - X_0} - c_{cL}(x)].\lambda(x)\} \\ X_{T+1} + (X_{T+1} - X_{L-1}).\{c_{cU}(x) + [\frac{X - X_{T+1}}{X_{L-1} - X_{T+1}} - c_{cU}(x)].\lambda(x)\} \end{cases} \quad (16)$$

$$\lambda(x) = \begin{cases} 1 - \mu & \text{for } \hat{a}(x) < \mu \\ (1 - k\mu) + k * \hat{a} & \text{otherwise} \end{cases}$$
$$\hat{a}(x) = \frac{\sigma^2(x)}{\sigma^2(x) + \varepsilon} \quad (17)$$

Where k is the sharpening parameter, which indicates the degree of sharpness. μ is the average of $\hat{a}(x)$ of the entire image. It is noted that $\hat{a}(x)$ has a high value in the edge region and low value in the flat region, and $\sigma^2(x)$ is the local variance of the input image in the guided filter window. The following algorithm clarifies the proposed approach.

The proposed algorithm

1. Obtain the image X
2. Divide the histogram into two sub histograms
   a. Calculate the primary value of the intensity threshold (X_T) based on the mean value of the image total illumination.
   b. Create an image histogram.
   c. Divide the histogram based on X_T into two sub-histograms.
   d. Compute the discrete entropy for each sub-histogram
3. Repeat step 2 until the difference in discrete entropy for each sub-histogram is minimized.
4. Calculate the probability distribution function (PDF) for each sub-section.
5. Calculate the plateau threshold for clipping PDF for each sub-section.
6. Clip the PDF of each sub-section by the plateau threshold.
7. Calculate the cumulative distribution function for each sub-section (CDF).
8. Calculate the transfer equalization function.

.

Figure 1. Samples of USC-SIPI dataset [51].

III. Laboratory Study

To evaluate the proposed method, eight other methods have been implemented for comparison. They are FPH [43], MMHE [44], WHE [45], AGCgw [46], AGClw [46], EEBHE [47], WCOGC [48], AGCHE [49], FHEW [50]. Additionally, the USC-SIPI dataset [51] was used for validation. Figure 1 shows samples of the mentioned dataset.

To evaluate the quality of the proposed approach, Shannon Entropy, Contrast to Noise Ratio (CNR) [52], Homogeneity, Perceptual Sharpness Index (PSI) [53] and Perceptual Image Quality Evaluator (PIQUE) [54] were used. Shannon entropy, as a no-reference-based metric measures the level of existing details in the image. Shannon entropy is shown in equation 18. $P(i)$ is the probability of the ith illumination in this equation.

[DOI: 10.52547/itrc.14.4.36]

$$E = -\sum_{i=0}^{255} P(i) \times log_2(P(i)) \quad (18)$$

The contrast-to-noise ratio is a reference-based metric with characteristics similar to the signal-to-noise ratio (SNR) that can evaluate the contrast level of an image relative to the noise level. The SNR value increases as the signal level increases. In the image, the signal level is proportional to the brightness level. As a result, for a washed-out image, the SNR value will be high due to high brightness values. Therefore, SNR cannot be used to control image quality. CNR is calculated according to equation 19, where μ_i is the average value of the image, μ_{ref} and σ_{ref} are the average brightness and standard deviation of the reference image, respectively.

$$CNR = \sigma_{ref}^{-1}(\mu_i - \mu_{ref}) \quad (19)$$

The homogeneity metric determines the probability that the illumination intensity of the pixels in the image is the same. High values of this metric indicate that the resulting image is more uniform. In other words, the process noise in image processing was negligible. Because if the aforementioned noise is effective, then noise values will reduce the homogeneity metric level by changing the images and causing small amount of reduction in the brightness values of the image pixels. Equation 20 shows the calculation of the homogeneity metric. In this equation, $p(i,j)$ is the brightness of the pixel at (i,j) coordinates.

$$Homogeneity = \sum_{i,j} \frac{p(i,j)}{1+|i-j|} \quad (20)$$

PSI is a metric for measuring image resolution based on its local gradient and is consistent with human perception. Equation 21 provides the aforementioned metric. $w_{up}(x,y)$ is the distance between the edge extracted from the image at the location (x,y) relative to the coordinates of the local maximum values $I_{max}(x,y)$. In a similar way, $w_{down}(x,y)$ is also defined as the distance between the edge extracted from the image at the location (x,y) relative to the coordinates of the local maximum values $I_{min}(x,y)$. Also, $\Delta\varphi(x,y)$ is the direction of the local gradient vector.

$$PSI = \begin{cases} w(x,y) - \dfrac{I_{max}(x,y) - I_{min}(x,y)}{w(x,y)} & if\ w(x,y) \geq 3 \\ w(x,y) & otherwise \end{cases} \quad (21)$$

$$w(x,y) = \frac{w_{up}(x,y) - w_{down}(x,y)}{\cos(\Delta\varphi(x,y))}$$

The PIQUE metric was chosen to evaluate the amount of distortion in the image regardless of the reference of the results based on human perception. This measure focuses on the salient regions of the image. In other words, in calculating this metric, the image is first divided into salient regions. Then, for each highlighted region, the mentioned metric is calculated locally. The final result is obtained by summing up the local results. Equation 22 provides the PIQUE calculation formula. N_{SA} is the number of salient regions, v_{blk} and σ_{blk} are the variance and standard deviation for each highlighted region, respectively. In addition, σ_{cen} and σ_{sur} are the standard deviation of the central part and the peripheral parts of the mentioned region, respectively.

$$PIQUE = \frac{(\sum_{K=1}^{N_{SA}} D_{SK}) + 1}{(N_{SA}+1)}$$

$$D_{SK} = \begin{cases} 1 & if\ \sigma_{blk} > 2\beta\ and\ \sigma_{pq} < T \\ v_{blk} & if\ \sigma_{blk} > 2\beta \\ 1 - v_{blk} & if\ \sigma_{pq} < T \end{cases} \quad (22)$$

$$\beta = \frac{\left|\dfrac{\sigma_{cen}}{\sigma_{sur}} - \sigma_{blk}\right|}{\max\left(\dfrac{\sigma_{cen}}{\sigma_{sur}}, \sigma_{blk}\right)}$$

The evaluation results were repeated on 49 images of the dataset. Two points are important in this experience. 1) The nature of the images in the dataset is quite different. Different results are due to the difference in the nature of the evaluated image. 2) Since each of the evaluation metrics measures the quality from its own perspective, it is necessary to calculate the resultant evaluation for the final ranking of the compared methods on each image. For any selected image, the desired resultant evaluation is the average performance rank of each method for any aforementioned metric. It should be mentioned that rank selection for evaluation, which is partially affected by the characteristics of the image, and has less impact on the final evaluation, helps to make significant differences in obtaining or not obtaining the result. As a result, the reference-evaluation of the unique features of each image that is reliable from a public perspective should be reported. After averaging the resulted ranks on all images of the dataset, the final rank is reported in Table 1.

TABLE I. RANKING OF THE PROPOSED METHOD ALONG WITH OTHER METHODS

Method	Rank on noise free images	Rank for Gaussian noise = 0.1	Rank for Gaussian noise = 0.3	Rank for Speckle noise = 0.1	Rank for Speckle noise = 0.3
FPH [43]	5	5	7	6	8
MMHE [44]	6	6	3	3	5
WHE [45]	10	10	9	10	9
AGCgw [46]	9	3	6	7	6
AGClw [46]	7	2	**1**	5	4
EEBHE [47]	2	7	5	2	2
WCOGC [48]	8	4	4	4	**1**
AGCHE [49]	3	9	10	8	7
FHEW [50]	4	8	8	9	10
EBHE (Proposed method)	**1**	**1**	2	**1**	3

In order to explain the results, two samples from the aforementioned dataset have been examined. Figure 2 compares the illumination correction results for the proposed method on an aerial image of a location with other methods. Also, the quantitative results of this comparison are presented in Table 2. Studying the table

[DOI: 10.52547/itrc.14.4.36]

shows that the proposed method ranks 2nd, 1st, 3rd, 3rd, and 4th in terms of entropy, PSI, PIQUE, CNR, and homogeneity. Also, in terms of running speed, the algorithm rank of the proposed method is 6th.

Figure 3 compares the illumination correction results for the proposed method on an aerial image of an aircraft with other methods. Also, the quantitative results of this comparison are presented in Table 3. Studying the table shows that the proposed method ranks 2nd, 1st, 1st, 4th, and 1st in terms of entropy, PSI, PIQUE, CNR, and homogeneity. Also, in terms of running speed, the rank of the algorithm of the proposed method is the 4th.

TABLE II. RESULTS OF COMPARING THE EVALUATION CRITERIA OF THE PROPOSED METHOD WITH OTHER METHODS ON NOISE-FREE IMAGE SAMPLE NUMBER 1

	Noise free image						Noisy image with Gaussian noise variance = 0.1						Noisy image with Gaussian noise variance = 0.3						Noisy image with impulse noise amplitude = 0.1						Noisy image with impulse noise amplitude = 0.3					
Method	**Runtime**	**Entropy**	**PSI**	**PIQUE**	**CNR**	**Homogeneity**	**Runtime**	**Entropy**	**PSI**	**PIQUE**	**CNR**	**Homogeneity**	**Runtime**	**Entropy**	**PSI**	**PIQUE**	**CNR**	**Homogeneity**	**Runtime**	**Entropy**	**PSI**	**PIQUE**	**CNR**	**Homogeneity**	**Runtime**	**Entropy**	**PSI**	**PIQUE**	**CNR**	**Homogeneity**
FPH [43]	0.09	7.05	0.41	15.44	302.87	0.85	0.07	7.34	0.56	65.66	475.89	0.62	0.09	6.92	0.61	65.97	459.28	0.64	0.08	6.87	0.60	57.06	470.18	0.75	0.07	6.06	0.81	77.94	634.61	0.58
MMHE [44]	0.43	7.35	0.43	15.47	98.44	0.86	0.37	7.58	0.57	65.46	156.15	0.62	0.64	7.25	0.53	66.16	148.29	0.65	0.36	7.17	0.60	62.29	161.14	0.75	0.38	6.31	0.74	79.23	215.91	0.58
WHE [45]	0.59	7.25	0.44	21.19	103.73	0.82	0.50	7.45	0.57	66.94	165.56	0.56	6.19	7.16	0.54	67.73	168.00	0.57	2.13	7.08	0.66	55.35	151.87	0.73	4.24	6.20	0.74	78.09	197.13	0.58
AGCgw [46]	6.24	7.41	0.44	16.72	104.66	0.84	6.68	7.69	0.54	68.19	162.24	0.57	6.90	7.33	0.52	67.31	160.98	0.62	5.53	7.25	0.62	56.73	160.61	0.74	5.23	6.40	0.77	78.23	210.36	0.58
AGCIw [46]	11.79	7.42	0.42	20.43	103.95	0.82	10.91	7.62	0.55	68.28	180.95	0.55	12.46	7.02	0.58	69.91	172.71	0.59	9.93	7.19	0.60	57.38	160.72	0.72	9.84	6.33	0.81	77.35	207.09	0.57
EEBHE [47]	0.61	7.42	0.44	23.45	111.49	0.80	0.50	7.69	0.55	66.35	173.09	0.55	0.65	5.47	0.58	64.73	147.37	0.66	0.50	7.27	0.59	51.89	150.92	0.72	0.48	6.52	0.73	77.84	195.04	0.60
WCOGC [48]	14.65	7.34	0.42	15.45	95.07	0.87	13.73	6.89	0.61	61.39	102.08	0.72	12.65	6.35	0.60	61.11	137.23	0.79	12.72	6.47	0.63	66.01	174.32	0.81	12.27	5.84	0.85	82.56	228.66	0.61
AGCHE [49]	0.12	5.65	0.47	38.31	187.08	0.92	0.19	6.28	0.54	53.12	326.39	0.75	0.09	6.49	0.62	60.04	430.65	0.66	0.11	5.59	0.75	71.15	506.66	0.84	0.09	5.07	0.89	91.77	649.69	0.71
FHEW [50]	0.43	7.07	0.43	22.90	321.25	0.82	0.61	6.98	0.55	63.73	442.55	0.65	0.34	5.67	0.60	54.60	321.11	0.82	0.36	6.64	0.72	61.71	483.02	0.76	0.33	5.85	0.89	84.58	637.62	0.64
EBHE (Proposed method)	0.60	7.67	0.42	22.43	300.73	0.84	0.56	7.81	0.50	54.93	419.51	0.63	0.68	7.30	0.53	64.02	459.51	0.66	0.56	7.55	0.58	50.50	498.08	0.72	0.53	6.63	0.69	71.95	612.65	0.57

[DOI: 10.52547/itrc.14.4.36]

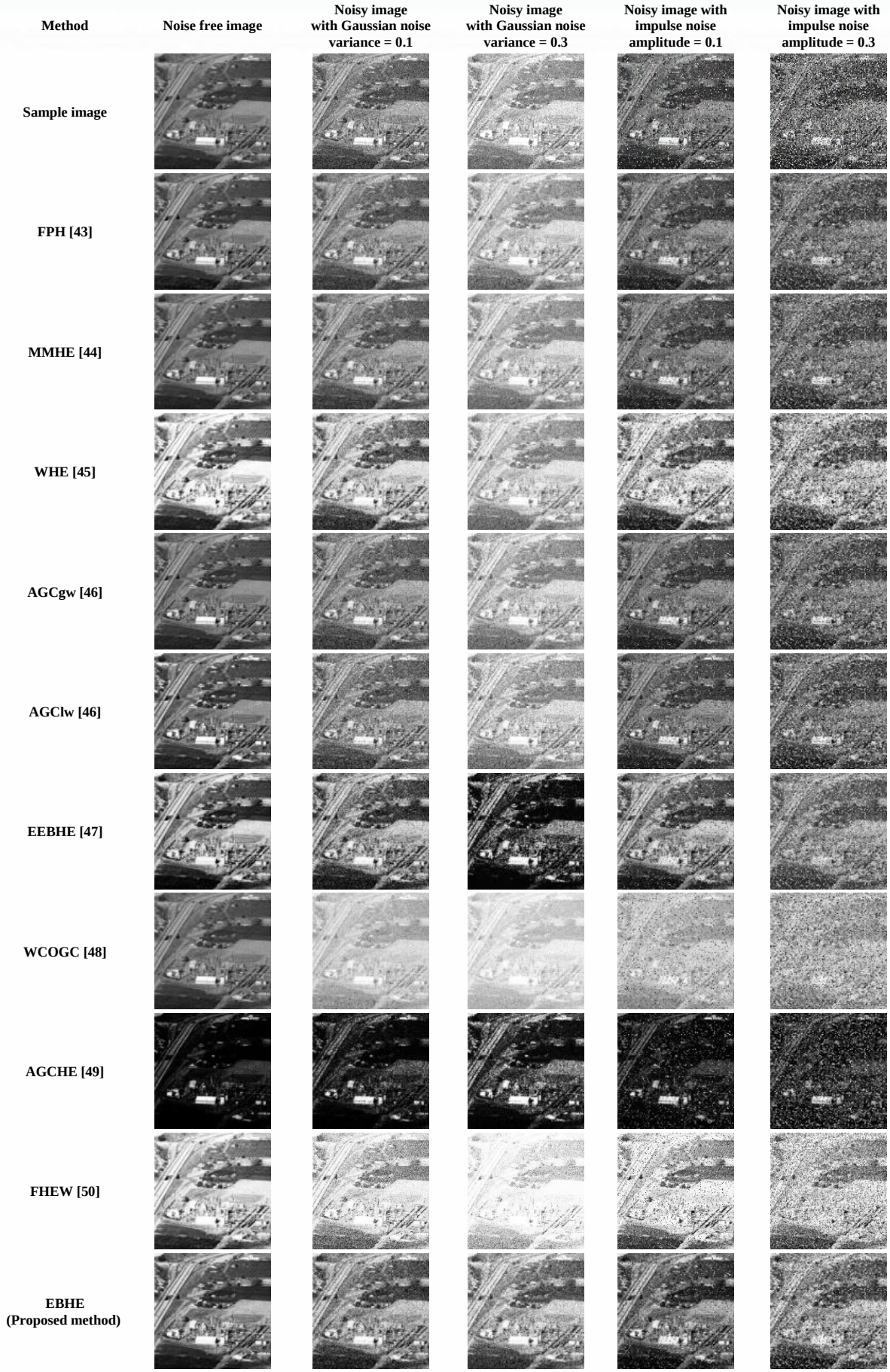

Figure 2. Visual comparison of illumination correction methods for noisy image sample number 1

[DOI: 10.52547/itrc.14.4.36]

TABLE III. RESULTS OF COMPARING THE EVALUATION CRITERIA OF THE PROPOSED METHOD WITH OTHER METHODS ON NOISE-FREE IMAGE SAMPLE NUMBER 2

	Noise free image						Noisy image with Gaussian noise variance = 0.1						Noisy image with Gaussian noise variance = 0.3						Noisy image with impulse noise amplitude = 0.1						Noisy image with impulse noise amplitude = 0.3					
Method	**Runtime**	**Entropy**	**PSI**	**PIQUE**	**CNR**	**Homogeneity**	**Runtime**	**Entropy**	**PSI**	**PIQUE**	**CNR**	**Homogeneity**	**Runtime**	**Entropy**	**PSI**	**PIQUE**	**CNR**	**Homogeneity**	**Runtime**	**Entropy**	**PSI**	**PIQUE**	**CNR**	**Homogeneity**	**Runtime**	**Entropy**	**PSI**	**PIQUE**	**CNR**	**Homogeneity**
FPH [43]	0.27	3.75	0.75	40.33	137.81	0.93	0.20	6.34	0.61	71.50	484.24	0.63	0.18	3.58	0.85	77.97	343.18	0.87	0.23	4.17	0.79	67.75	546.12	0.80	0.21	3.95	0.80	82.64	692.02	0.62
MMHE [44]	2.15	4.01	0.75	20.96	20.74	0.96	1.32	6.85	0.58	72.69	97.59	0.64	1.34	4.09	0.81	78.86	47.25	0.88	1.29	4.18	0.79	75.27	185.80	0.83	1.30	3.99	0.83	87.28	231.04	0.63
WHE [45]	3.10	3.99	0.71	38.99	49.05	0.91	4.03	6.73	0.66	74.52	181.86	0.51	4.93	3.87	0.86	83.90	152.85	0.70	3.56	4.16	0.77	60.76	167.66	0.80	5.54	3.97	0.83	83.42	215.26	0.62
AGCgw [46]	29.12	4.15	0.77	20.48	31.01	0.96	20.10	6.96	0.62	73.29	119.38	0.62	20.13	4.12	0.88	78.77	86.01	0.87	20.04	4.91	0.77	74.51	185.97	0.83	19.98	4.92	0.84	86.91	230.97	0.63
AGClw [46]	55.62	5.37	0.75	25.26	36.84	0.94	38.78	6.67	0.63	74.76	139.81	0.59	37.86	3.84	0.93	83.57	101.74	0.84	38.41	5.38	0.72	72.54	185.49	0.82	38.30	4.89	0.83	86.49	230.60	0.61
EEBHE [47]	2.24	4.77	0.74	59.78	65.43	0.80	1.90	6.76	0.64	77.59	199.00	0.48	1.81	4.12	0.00	87.85	118.12	0.54	1.72	4.20	0.74	58.87	154.71	0.72	1.73	4.75	0.81	76.97	209.56	0.60
WCOGC [48]	28.03	3.93	0.70	21.28	47.12	0.95	23.38	6.82	0.60	75.20	186.35	0.51	23.82	3.98	0.84	85.93	169.43	0.55	23.31	4.14	0.75	75.13	176.16	0.82	24.10	3.94	0.82	86.14	220.32	0.63
AGCHE [49]	0.38	3.94	0.73	35.63	154.72	0.92	0.35	6.68	0.67	72.96	559.00	0.50	0.33	4.04	0.87	84.99	498.04	0.58	0.29	4.11	0.77	67.17	507.47	0.79	0.30	3.93	0.77	83.84	655.25	0.60
FHEW [50]	1.59	3.60	0.78	37.27	48.69	0.99	1.33	4.90	0.69	56.17	155.48	0.94	1.32	2.07	0.85	73.23	87.30	0.98	1.24	4.06	0.92	73.51	531.29	0.90	1.27	3.92	1.00	95.01	690.21	0.77
EBHE (Proposed method)	1.78	6.83	0.54	12.38	162.24	0.90	1.13	7.26	0.64	64.24	410.93	0.63	0.94	4.24	0.87	76.18	321.50	0.83	1.13	6.73	0.71	52.22	528.19	0.77	1.01	5.97	0.94	73.25	645.38	0.62

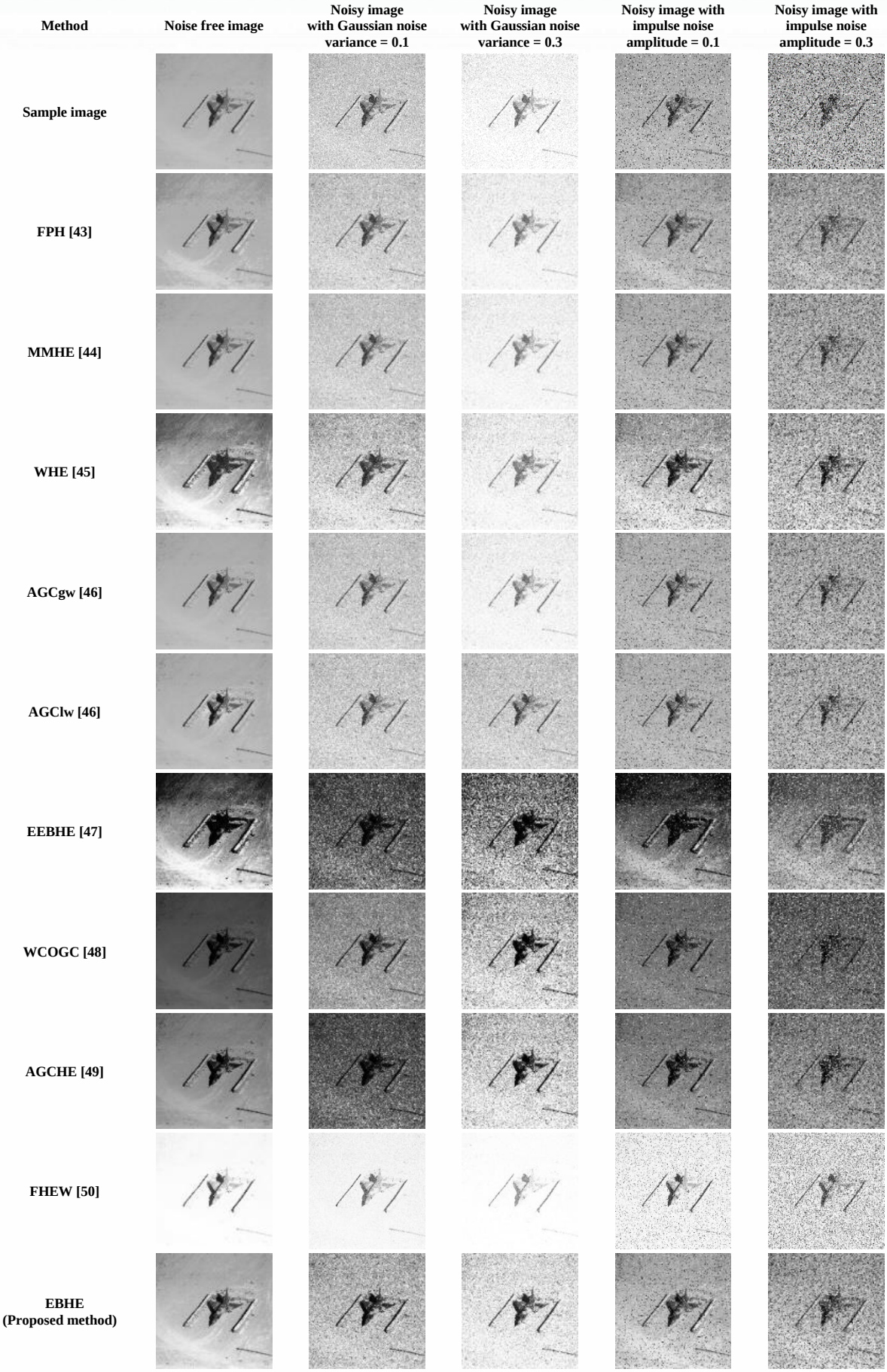

Figure 3. Visual comparison of illumination correction methods for noisy image sample number 2.

[DOI: 10.52547/itrc.14.4.36]

IV. Conclusion

The purpose of this paper was to investigate the equalization of the bi-histogram with the level of entropy-based plateau. Firstly, through the application of the mean brightness as a primary threshold of total image pixels, the input histogram is divided into two separate sub-histograms. Secondly, the mentioned threshold is updated so that it minimizes the difference value of discrete entropy between each section. Secondly, to prevent unnecessary enhancement by the consideration of the measured plateau value, the sub-histograms are clipped. Finally, the image intensity is stretched based on the cumulative distribution function. Comparing with other two-section methods of preserving brightness of the histogram equalization, the laboratory results show that the proposed method produce better enhancement results, especially in the presence of noise.

References

[1] [S. H. Lim, N. A. Mat Isa, C. H. Ooi, and K. K. V. Toh, "A new histogram equalization method for digital image enhancement and brightness preservation," Signal, Image Video Process., vol. 9, no. 3, pp. 675–689, 2015, doi: 10.1007/s11760-013-0500-z.

[2] M. F. Khan, X. Ren, and E. Khan, "Semi dynamic fuzzy histogram equalization," Optik (Stuttg)., vol. 126, no. 21, pp. 2848–2853, 2015, doi: 10.1016/j.ijleo.2015.07.036.

[3] H. Ibrahim and N. S. P. Kong, "Brightness preserving dynamic histogram equalization for image contrast enhancement," IEEE Trans. Consum. Electron., vol. 53, no. 4, pp. 1752–1758, Nov. 2007, doi: 10.1109/TCE.2007.4429280.

[4] M. Veluchamy and B. Subramani, "Image contrast and color enhancement using adaptive gamma correction and histogram equalization," Optik (Stuttg)., vol. 183, no. X, pp. 329–337, 2019, doi: 10.1016/j.ijleo.2019.02.054.

[5] J. Mun, Y. Jang, Y. Nam, and J. Kim, "Edge-enhancing bi-histogram equalisation using guided image filter," J. Vis. Commun. Image Represent., vol. 58, no. 21 Dec, pp. 688–700, Jan. 2019, doi: 10.1016/j.jvcir.2018.12.037.

[6] D. Tohl and J. S. J. Li, "Contrast enhancement by multi-level histogram shape segmentation with adaptive detail enhancement for noise suppression," Signal Process. Image Commun., vol. 71, no. October 2018, pp. 45–55, 2019, doi: 10.1016/j.image.2018.10.011.

[7] A. Hosni, C. Rhemann, M. Bleyer, C. Rother, and M. Gelautz, "Fast cost-volume filtering for visual correspondence and beyond," IEEE Trans. Pattern Anal. Mach. Intell., vol. 35, no. 2, pp. 504–511, 2013, doi: 10.1109/TPAMI.2012.156.

[8] [8] K. He, J. Sun, and X. Tang, "Guided image filtering," IEEE Trans. Pattern Anal. Mach. Intell., vol. 35, no. 6, pp. 1397–1409, 2013, doi: 10.1109/TPAMI.2012.213.

[9] A. Kaur and C. Singh, "Contrast enhancement for cephalometric images using wavelet-based modified adaptive histogram equalization," Appl. Soft Comput. J., vol. 51, no. 29, pp. 180–191, 2017, doi: 10.1016/j.asoc.2016.11.046.

[10] Y. Yang, Z. Su, and L. Sun, "Medical image enhancement algorithm based on wavelet transform," Electron. Lett., vol. 46, no. 2, pp. 120–121, 2010, doi: 10.1049/el.2010.2063.

[11] A. S. Parihar, O. P. Verma, and C. Khanna, "Fuzzy-Contextual Contrast Enhancement," IEEE Trans. Image Process., vol. 26, no. 4, pp. 1810–1819, Apr. 2017, doi: 10.1109/TIP.2017.2665975.

[12] B. Xiao, H. Tang, Y. Jiang, W. Li, and G. Wang, "Brightness and contrast controllable image enhancement based on histogram specification," Neurocomputing, vol. 275, no. 5, pp. 2798–2809, 2018, doi: 10.1016/j.neucom.2017.11.057.

[13] S. Agrawal, R. Panda, P. K. Mishro, and A. Abraham, "A novel joint histogram equalization-based image contrast enhancement," J. King Saud Univ. - Comput. Inf. Sci., vol. 5, no. xxxx, p. 28, 2019, doi: 10.1016/j.jksuci.2019.05.010.

[14] Q. Wang and R. Ward, "Fast image/video contrast enhancement based on WTHE," in 2006 IEEE 8th Workshop on Multimedia Signal Processing, MMSP 2006, 2006, vol. 53, no. 4, pp. 338–343, doi: 10.1109/MMSP.2006.285326.

[15] T. Celik, "Two-dimensional histogram equalization and contrast enhancement," Pattern Recognit., vol. 45, no. 10, pp. 3810–3824, 2012, doi: 10.1016/j.patcog.2012.03.019.

[16] Y. F. Liu, J. M. Guo, and J. C. Yu, "Contrast Enhancement Using Stratified Parametric-Oriented Histogram Equalization," IEEE Trans. Circuits Syst. Video Technol., vol. 27, no. 6, pp. 1171–1181, 2017, doi: 10.1109/TCSVT.2016.2527338.

[17] B. Gupta and T. K. Agarwal, "Linearly quantile separated weighted dynamic histogram equalization for contrast enhancement," Comput. Electr. Eng., vol. 62, no. 3, pp. 360–374, 2017, doi: 10.1016/j.compeleceng.2017.01.010.

[18] X. Wang and L. Chen, "An effective histogram modification scheme for image contrast enhancement," Signal Process. Image Commun., vol. 58, no. 8, pp. 187–198, 2017, doi: 10.1016/j.image.2017.07.009.

[19] J. Shin and R.-H. Park, "Histogram-Based Locality-Preserving Contrast Enhancement," IEEE Signal Process. Lett., vol. 22, no. 9, pp. 1293–1296, 2015.

[20] Y. Chang, C. Jung, P. Ke, H. Song, and J. Hwang, "Automatic Contrast-Limited Adaptive Histogram Equalization with Dual Gamma Correction," IEEE Access, vol. 6, no. 25 Jan, pp. 11782–11792, 2018, doi: 10.1109/ACCESS.2018.2797872.

[21] J. A. Stark, "Adaptive image contrast enhancement using generalizations of histogram equalization," IEEE Trans. Image Process., vol. 9, no. 5, pp. 889–896, 2000, doi: 10.1109/83.841534.

[22] Y. Wang and Z. Pan, "Image contrast enhancement using adjacent-blocks-based modification for local histogram equalization," Infrared Phys. Technol., vol. 86, no. X, pp. 59–65, 2017, doi: 10.1016/j.infrared.2017.08.005.

[23] J. Jasmine and S. Annadurai, "Real time video image enhancement approach using particle swarm optimisation technique with adaptive cumulative distribution function-based histogram equalization," Meas. J. Int. Meas. Confed., vol. 145, no. X, pp. 833–840, 2019, doi: 10.1016/j.measurement.2018.12.105.

[24] K. Singh and R. Kapoor, "Image enhancement via Median-Mean Based Sub-Image-Clipped Histogram Equalization," Optik (Stuttg)., vol. 125, no. 17, pp. 4646–4651, 2014, doi: 10.1016/j.ijleo.2014.04.093.

[25] S. Der Chen and A. R. Ramli, "Minimum mean brightness error bi-histogram equalization in contrast enhancement," IEEE Trans. Consum. Electron., vol. 49, no. 4, pp. 1310–1319, 2003, doi: 10.1109/TCE.2003.1261234.

[26] M. Kim and M. G. Chung, "Recursively separated and weighted histogram equalization for brightness preservation and contrast enhancement," IEEE Trans. Consum. Electron., vol. 54, no. 3, pp. 1389–1397, 2008, doi: 10.1109/TCE.2008.4637632.

[27] C. H. Ooi, N. P. Kong, and H. Ibrahim, "Bi-histogram equalization with a plateau limit for digital image enhancement," IEEE Trans. Consum. Electron., vol. 55, no. 4, pp. 2072–2080, Nov. 2009, doi: 10.1109/TCE.2009.5373771.

[28] S. Der Chen and A. R. Ramli, "Contrast enhancement using recursive mean-separate histogram equalization for scalable brightness preservation," IEEE Trans. Consum. Electron., vol. 49, no. 4, pp. 1301–1309, 2003, doi: 10.1109/TCE.2003.1261233.

[29] A. S. Parihar and O. P. Verma, "Contrast enhancement using entropy-based dynamic sub-histogram equalisation," IET Image Process., vol. 10, no. 11, pp. 799–808, Nov. 2016, doi: 10.1049/iet-ipr.2016.0242.

[30] E. F. Arriaga-Garcia, R. E. Sanchez-Yanez, and M. G. Garcia-Hernandez, "Image enhancement using Bi-histogram equalization with adaptive sigmoid functions," in CONIELECOMP 2014 - 24th International Conference on Electronics, Communications and Computers, 2014, vol. X, no. 26, pp. 28–34, doi: 10.1109/CONIELECOMP.2014.6808563.

[31] J. R. Tang and N. A. Mat Isa, "Bi-histogram equalization using modified histogram bins," Appl. Soft Comput. J., vol. 55, no. 27 Jan, pp. 31–43, 2017, doi: 10.1016/j.asoc.2017.01.053.

[32] N. Sengee and H. K. Choi, "Brightness preserving weight clustering histogram equalization," IEEE Trans. Consum.

[DOI: 10.52547/itrc.14.4.36]

Electron., vol. 54, no. 3, pp. 1329–1337, 2008, doi: 10.1109/TCE.2008.4637624.
[33] G. Rajagopal, "Contrast Enhancement Using Bi-Histogram Equalization With Brightness Preservation," Int. J. Basic Appl. Sci., vol. 4, no. May, pp. 2–6, 2013.
[34] S. C. F. Lin et al., "Image enhancement using the averaging histogram equalization (AVHEQ) approach for contrast improvement and brightness preservation," Comput. Electr. Eng., vol. 46, no. 12, pp. 356–370, 2015, doi: 10.1016/j.compeleceng.2015.06.001.
[35] Li. Canlin, Liu. Jinhua, Zhu. Jinjuan, Zhang .Weizheng, Bi. Lihua, "Mine image enhancement using adaptive bilateral gamma adjustment and double plateaus histogram equalization," Multimed Tools Appl, vol. 81, pp. 12643–12660, Feb.2022, doi: 10.1007/s11042-022-12407-z.
[36] B. Subramani, M. Veluchamy, "Fuzzy Gray Level Difference Histogram Equalization for Medical Image Enhancement," J Med Syst, vol.44, no.103 ,Apr. 2020, doi: 10.1007/s10916-020-01568-9.
[37] Z. Huang, Z. Wang, Z. hang, Q. Li, Y. Shi, "Image enhancement with the preservation of brightness and structures by employing contrast limited dynamic quadri-histogram equalization," Journal Pre-proof, vol. 226, no. 165877, Jan. 2021, doi: 10.1016/j.ijleo.2020.165877.
[38] A. Paul, P. Bhattacharya, SP. Maity, "Histogram modification in adaptive bi-histogram equalization for contrast enhancement on digital images," International Journal for Light and Electron Optics, vol. 259, Jun. 2022, doi: 10.1016/j.ijleo.2022.168899.
[39] JB. Rao, K V G. Srinivas, AS. kumar, JB . Seventline, "Bi Histogram Equalization Based Image Enhancement with Bicubic Interpolation," The Electrochemical Society, vol. 107, no. 1, Apr.2022, doi:10.1149/10701.1441ecst.
[40] K. Acharya, D. Ghoshal, "Standard Deviation and Mode Based Bi-Histogram Equalization Algorithm for Image Enhancement," SSRN Electronic, Jan.2021, doi: 10.2139/ssrn.3768018.
[41] T. Kim and J. Paik, "Adaptive contrast enhancement using gain-controllable clipped histogram equalization," IEEE Trans. Consum. Electron., vol. 54, no. 4, pp. 1803–1810, 2008, doi: 10.1109/TCE.2008.4711238.
[42] M. Zarie, H. Hajghassem, and A. E. Majd, "Contrast Enhancement Using Triple Dynamic Clipped Histogram Equalization Based on Mean or Median," Opt. - Int. J. Light Electron Opt., vol. 45, no. 12, pp. 41–57, 2018, doi: 10.1016/j.ijleo.2018.08.082.
[43] H. Garud, D. Sheet, A. Suveer, P. K. Karri, A. K. Ray, M. Mahadevappa, J. Chatterjee, "Brightness preserving contrast enhancement in digital pathology," 2011 International Conference on Image Information Processing, 03-05 November, 2011.
[44] K. Singha, R. Kapoor, "Image enhancement via Median-Mean Based Sub-Image-Clipped Histogram Equalization," Optik, Volume 125, Issue 17, September 2014, Pages 4646-4651.
[45] H. Lidong, Z. Wei, W. Jun, S. Zebin, "Combination of contrast limited adaptive histogram equalisation and discrete wavelet transform for image enhancement, " IET image processing, Volume 9, Issue 10, October, 2015.
[46] Z. Huanga, T. Zhang, Q. Li, H. Fang, "Adaptive gamma correction based on cumulative histogram for enhancing near-infrared images, " Infrared Physics & Technology, Volume 79, November 2016, Pages 205-215.
[47] J. Mun, Y. Jang, Y. Nam, J. Kim, "Edge-enhancing bi-histogram equalisation using guided image filter," Journal of Visual Communication and Image Representation, Volume 58, January 2019, Pages 688-700.
[48] Y. Zhou, C. Shi, B. Lai, G. Jimenez, "Contrast enhancement of medical images using a new version of the World Cup Optimization algorithm, " Aims and Scope Quantitative Imaging in Medicine and Surgery, Vol 9, No 9, September 2019.
[49] M. Veluchamy, B. Subramani, "Image contrast and color enhancement using adaptive gamma correction and histogram equalization," Optik, Volume 183, April 2019, Pages 329-337.
[50] K. Mayathevar, M. Veluchamy, B. Subramani, "Fuzzy color histogram equalization with weighted distribution for image enhancement, " Optik, Volume 216, August 2020.
[51] U.-S. Database, "Http://sipi.usc.edu/database," 2017. http://sipi.usc.edu/database.
[52] Y. Zhou, C. Shi, B. Lai, and G. Jimenez, "Contrast enhancement of medical images using a new version of the World Cup Optimization algorithm," Quant. Imaging Med. Surg., vol. 9, no. 9, pp. 1528–1547, 2019.
[53] C. Feichtenhofer, H. Fassold, P. Schallauer "A perceptual image sharpness metric based on local edge gradient analysis", IEEE Signal Processing Letters, 20 (4), 379-382, 2013.
[54] N. Venkatanath, D. Praneeth, Bh. M. Chandrasekhar, S. S. Channappayya, and S. S. Medasani. "Blind Image Quality Evaluation Using Perception Based Features", In Proceedings of the 21st National Conference on Communications (NCC). Piscataway, NJ: IEEE, 2015.

Vida Safardoulabi is a Ph.D. candidate in Computer Artificial Intelligence at the Department of Computer Engineering, Islamic Azad University (IAU), South Tehran Branch, Tehran, Iran. She obtained M.Sc. (Artificial Intelligence) in 2020 from IAU, South Tehran Branch, Tehran, Iran. Her main research interests are in the field of Machine Vision and Image Processing.

Kambiz Rahbar is an Associate Professor of Computer Engineering at the Department of Computer Engineering, Islamic Azad University (IAU), South Tehran Branch, Tehran, Iran. He obtained Ph.D. (Software Systems) in 2012 from IAU, Science and Research Branch, Tehran, Iran. His main research interests are in the field of Machine Vision and Image Processing.

[DOI: 10.52547/itrc.14.4.36]